

K. JAGIELSKA-WIADEREK*, H. BALA*, P. WIECZOREK**, J. RUDNICKI***, D. KLIMECKA-TATAR*

CORROSION RESISTANCE DEPTH PROFILES OF NITRIDED LAYERS ON AUSTENITIC STAINLESS STEEL PRODUCED AT ELEVATED TEMPERATURES

PROFILE GŁĘBOKOŚCIOWE ODPORNOŚCI KOROZYJNEJ AZOTOWANEJ W PODWYŻSZONEJ TEMPERATURZE NIERDZEWNEJ STALI AUSTENITYCZNEJ

Electrochemical polarisation characteristics of glow-discharge, high-temperature (520°C) nitrided AISI 321 steel are presented. The evaluation of the corrosion resistance of nitrided stainless steel was carried out by using the so called progressive thinning method, consisting in determination of polarisation characteristics on increasingly-deeper situated regions of the top layer. This method made it possible to determine changes in particular corrosion parameters read out from potentiokinetic polarisation curves, thus enabling the depth profiles of these parameters. The resistance of the AISI 321 steel against acid corrosion was determined in acidified 0.5M sulphate solution. The thickness of the nitrided layer has been evaluated on the basis of microhardness and chemical analysis on the cross section of the surface layer. The corrosion rate within the outer layers of the nitrided AISI 321 stainless steel is approximately 3-10 times as high as that of the matrix. The passive state characteristics of the treated layers are also worsened, which is manifested by a rapid increase in the critical passivation current and current density within the passive range.

Keywords: corrosion resistance, depth profile, austenitic steel, glow-discharge nitriding

W pracy przedstawiono potencjokinetyczne krzywe polaryzacyjne austenitycznej stali 1H18N9T poddanej wysokotemperaturowemu azotowaniu jarzeniowemu. Dla określenia głębokościowych charakterystyk korozyjnych stali 1H18N9T wykorzystano metodę postępującego ścieniania, która polega na wykonywaniu polaryzacyjnych testów korozyjnych na coraz głębiej położonych obszarach warstwy wierzchniej. Metoda ta pozwoliła na określenie zmian poszczególnych charakterystycznych parametrów korozyjnych odczytywanych z potencjokinetycznych krzywych polaryzacji, a co za tym idzie – umożliwiła wykreślenie profili głębokościowych tych parametrów. Badania potencjokinetyczne wykonano w 0,5M roztworze siarczanowym zakwaszonym do $\text{pH} = 1$. Grubość powstałej warstwy oceniano na podstawie analizy liniowej zawartości pierwiastków oraz mikrotwardości na przekroju poprzecznym obrobionego cieplnie materiału.

Szybkość korozji ogólnej obrobionych cieplno-chemicznie warstw zewnętrznych stali 1H18N9T w zakwaszonym roztworze siarczanowym jest 3-10-krotnie większa niż szybkość korozji osnowy. Pogorszenie charakterystyk stanu pasywnego azotowanej stali uwidacznia się przez wzrost wartości krytycznego prądu pasywacji oraz minimalnego prądu w zakresie pasywnym.

1. Introduction

Among numerous variants of thermo-chemical treatment of utility alloys, the operations of nitriding, carbonitriding and carburizing enjoy the greatest popularity. They have been used successfully for a long time, not only for the steel grades designed especially for this purpose [1,2], but also for steels of special properties, which include stainless and acid resistant steels [3,4]. The excellent corrosion resistance of Cr-Ni stainless steels in many aggressive environments results from outstanding

properties of passive layers spontaneously formed on surface of these steels, containing mainly Cr_2O_3 , Fe_2O_3 and NiO oxides and also NiM_2O_4 spinels ($M \equiv \text{Cr}$ or Fe) and having strongly ionic insulating properties [5,6]. The high-chromium (and nickel) stainless steel are not stable in strong oxidizing environments because of transpassivation of steel constituents (mainly Cr, but also Ni) [5,7]. The 18Cr-8Ni steels start transpassivation in acid solutions at 1.1V i.e. ca. 0.9V vs Ag/AgCl (SSE) electrode and gets into the secondary passive region at about 1.3V (SSE) [5,8]. Secondary passivation currents are usually

* DEPARTMENT OF CHEMISTRY, CZESTOCHOWA UNIVERSITY OF TECHNOLOGY, 42-200 CZESTOCHOWA 19 ARMII KRAJOWEJ AV., POLAND

** INSTITUTE OF MATERIALS ENGINEERING, CZESTOCHOWA UNIVERSITY OF TECHNOLOGY, 42-200 CZESTOCHOWA 19 ARMII KRAJOWEJ AV., POLAND

*** FACULTY OF MATERIALS SCIENCE AND ENGINEERING, WARSAW UNIVERSITY OF TECHNOLOGY, 02-507 WARSAW, POLAND

1-2 orders of magnitude higher than the currents in passive range. This is because of preferential dissolution of Cr and Ni oxides in transpassive range with formation of soluble CrO_4^{2-} and NiO_4^{2-} agents and enrichment of the passive layer with Fe_2O_3 and Fe_3O_4 oxides [5,7].

It is well known that both nitrogen and carbon are austenite-stabilizing elements, which shift the range of austenite occurrence towards higher chromium contents [9]. In austenitic steels, nitrogen is an element that effectively hardens the steels without causing any significant reduction in their elongation and reduction of cross-section area in tensile test. Steels with enhanced nitrogen content are characterized by a higher tensile strength, a higher yield point and an increased crack propagation resistance factor [10,11]. There are exceptionally many divergent views in literature on the corrosion resistance of nitrided high-chromium steels [12-14]. According to the review study by Sura [15], nitriding may either increase or decrease the corrosion resistance of high-chromium steels, depending on the chemical composition and structure of the material. In particular, chromium and nickel are considered to exhibit greater affinity to nitrogen than iron, so one should expect engagement of these elements in formation of Cr-N and Ni-N compounds and precipitates, resulting in depleting of steel matrix with these elements and, consequently, worsening of surface passivating properties. In paper [16] it was found that high temperature nitriding of AISI 316L steel (550°C) produces chromium and iron nitrides in outer zone of the surface layers. Low-temperature nitriding (380-450°C) produces a supersaturated solid solution of nitrogen in austenite (so called S-phase) with up to *ca.* 13 mass % N [16-19] which is detrimental for the high-chromium steel in acidified solutions (pH=3) but advantageous in neutral solutions (pH=6) [17]. The S-phase is considered to be very well corrosion resistant [18-20], although there exist also different views [21]. It is well known that the glow discharge nitriding of the austenitic stainless steels at temperatures below 450°C is useful process for improving their wear and corrosion resistance [13, 16, 30, 31].

Both the strength and the corrosion resistance of stainless steels are a resultant of the interactions between forming precipitates and the matrix and engagement of large amounts of Cr (and Ni) in these precipitates. Therefore, the present study undertakes investigation aimed at the understanding of changes in corrosion resistance on the cross-section of the nitrided top layer.

2. Experimental procedure

The subject of testing was AISI 321 austenitic steel of the following chemical composition (mass

%) : 0.023C, 17.35Cr, 9.70Ni, 1.97Mn, 0.13Co, 0.15Ti, 0.44Si, 0.034N and 0.032P. The test material was subjected to glow discharge nitriding in an N_2/H_2 atmosphere with the volume ratio of 1:1 at a elevated temperature of 520°C. The surface treatment parameters were selected so as to obtain of a relatively thick surface layer that would have clearly diversified properties on its cross-section. It should be stressed that these parameters were not optimal from the corrosion point of view, since the tests carried out were model ones and cognitive in assumption and their crucial goal was just to obtain adequately thick nitrided layers. From cognitive point of view, there is essential to explain the mechanism and a role of nitride compounds and precipitates in corrosion process of nitrided stainless steels. Since the presence and concentration of individual phase change with a distance from the nitrided surface, there is of great interest to register deep profiles of corrosion parameters across the steel surfacial layers. Solution of presented task is possible by the use of the progressive thinning method which has been described in details and applied in our earlier papers [22-25].

Metallographic examination was carried out on Adler solution specimens using a Neophot 32 optical microscope. Microhardness was measured by the Vickers method with a load of 0,49 N (HV0,05) along normal to the nitrided surface on the cross-section of samples.

The examination of chemical composition (being linear in the layer cross-section and punctual in the material grains) was carried out with the use of electron scanning microscope HITACHI S-3500N equipped with an EDS camera (Thermo NORAN VANTAGE).

2.1. Potentiokinetic polarisation tests

Potentiokinetic polarization tests were carried out in 0.5M sulphate solution acidified to pH = 1. Electrodes for the polarization testing of the nitrided AISI 321 steel had the form of rotating discs with the operating surface area of 0.2 cm². Prior to each potentiokinetic measurement, parallel electrode layers of a thickness of $4 \div 10$ μm were taken off by polishing (waterproof emery paper, grade 1000), while proceeding from the surface into the depth of the steel. After polishing, the electrodes were rinsed with water, degreased with alcohol and dried. The thickness of the layers ground off was determined from the mass loss of the examined disc electrode in relation to its initial mass, established with an accuracy of ±0.02 mg. The methodology described above [22-25] is called the *progressive thinning method*. The potentiokinetic polarization curves have been measured at a temperature of $25 \pm 0.1^\circ\text{C}$, with the disc rotation speed equal to 12 rps and with the potential scan rate of 10 mVs⁻¹, using the potential scanning from $E_{\text{start}} = -1.0\text{V}$ to the value of

$E_{\text{end}} = 1.9\text{V}$. The values of all the electrode potentials are expressed versus the silver/silver chloride reference electrode (SSE) for which $E_{\text{Ag/AgCl}}^0 = 0.22\text{V}$. The corrosion currents have been determined from polarization resistance (R_p) data [26]. Assuming that Tafel slopes are analogous as for iron in sulphate solutions (i.e. $b_a = 0.04$

and $b_c = 0.12\text{ V}$) [27] one can find that $i_{\text{cor}} = 0.013 R_p^{-1}$ where i_{cor} is expressed in Acm^{-2} and R_p in Ωcm^2 .

3. Results and discussion

The microstructure of the nitrated surface layer on AISI 321 steel is shown in Fig. 1.

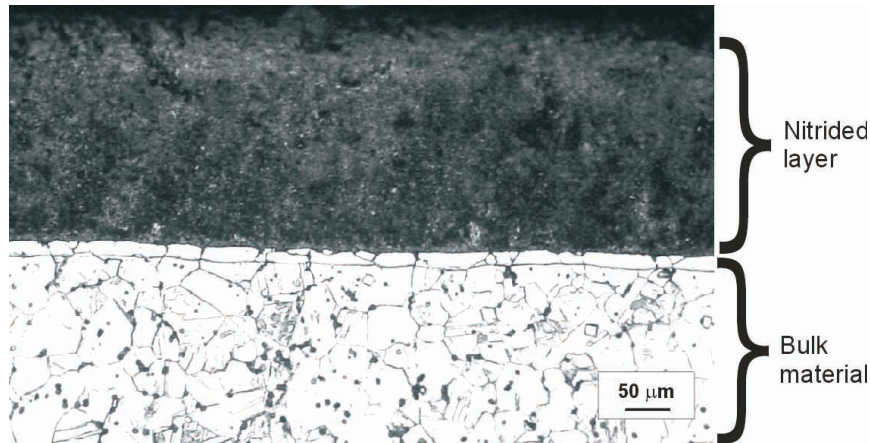


Fig. 1. Microstructure of the nitrated surface layer formed on AISI 321 austenitic stainless steel at temperature 520°C

As can be seen from Fig. 1, the nitrated layer extends to a depth of approx. $260\ \mu\text{m}$. Up to this depth, one can observe a region of a microstructure distinctly different from that of the bulk material. Down to a comparable depth, an increased nitrogen content is also observed, and the examination of chemical composition on the top layer cross-section shows that the nitrogen content changes in the nitride layer from ca 5 mass % in the outer layer zone (up to $30\ \mu\text{m}$ – zone depleted also with Cr, Ni, and Fe) to 2.5 mass % at the nitrated layer/substrate interface (Fig. 2). Similarly, down to a depth of $260\ \mu\text{m}$, the material microhardness on the cross-section of the nitrated AISI 321 steel layer rapidly changes. As can be seen in Fig. 3, the microhardness varies from approx. 1400 HV0.05 on the outer layer surface, through ca. 1100 HV0.05 within the layer, to 200 HV0.05 in the core.

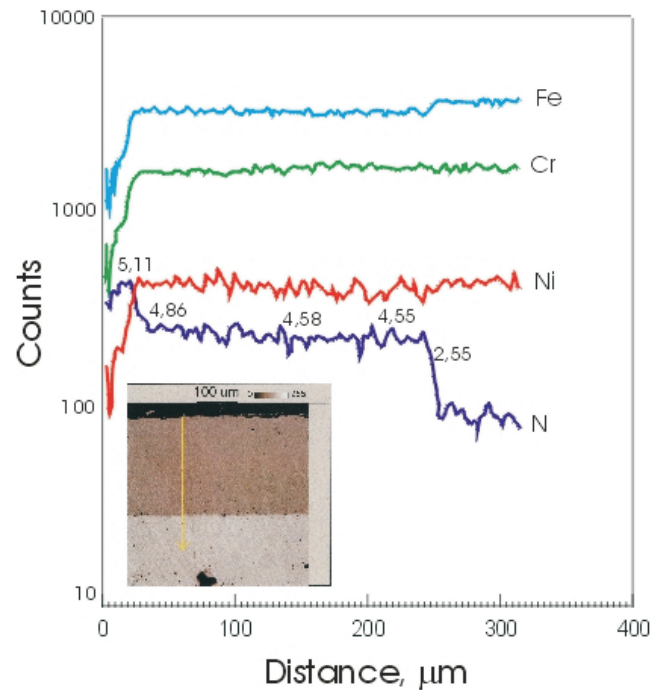


Fig. 2. Distributions of the chemical elements: Fe, Ni and N on the cross section of the nitrated layer. The numbers at the N-distribution curve denote nitrogen mass percentage

As it was already mentioned, the comparatively thick ($260\ \mu\text{m}$) a top nitrated layer was formed owing to the application of suitably selected parameters

of thermo-chemical treatment. It should be stressed here that, in practice, much thinner layers, of a thickness less than 30 μm , are produced using typical (low-temperature) technologies of nitriding of austenitic steels [28, 29].

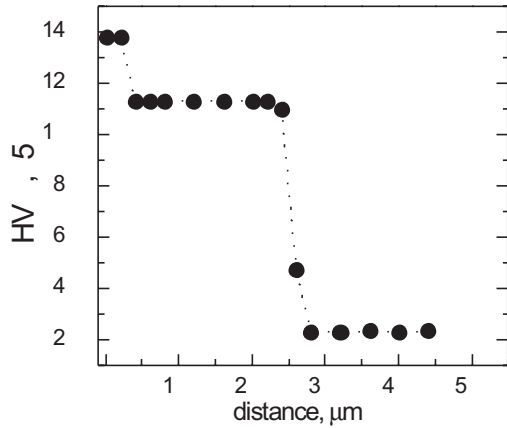


Fig. 3. Microhardness of nitrided AISI 321 steel as a function of distance from the surface

Fig.4 presents a set of potentiodynamic polarization curves measured for several distances from the initial sur-

face of nitrided steel. The curve series characterize the corrosion behaviour of the material in several different depths relating to the initial sample surface which had been previously subjected to the nitriding. To make the plots more readable only the polarization curves for a few depths have been chosen out of tens of curves obtained for the consecutive layers removed. The curves presented in Fig.4. can be divided into two groups. The first one (type I) – has a very wide active peak and limiting-like anodic current at potential range from -0.2 to $+0.5\text{V}$ (plot close to pure iron in acidified solutions). The second group of curves (type II) with a narrow and a small anodic peak (at $E \approx -0.3\text{V}$) and low anodic current density within passive range (on the order of 0.1 mAcm^{-2}) corresponds to pure chromium and high-chromium steels (e.g. AISI 316, AISI 321 etc). It should be noted that curves of type I exhibit continuous increase (from *ca.* 1 to *ca.* 200 mAcm^{-2}) of anodic currents in passive range with increase of potential, so one should call it "tendency to passivation" rather than passivation. Both types of polarization curves show transpassive region between 0.9 and 1.3V, followed by secondary passivation (*ca.* 1.4V) and oxygen evolution ($>1.5\text{V}$).

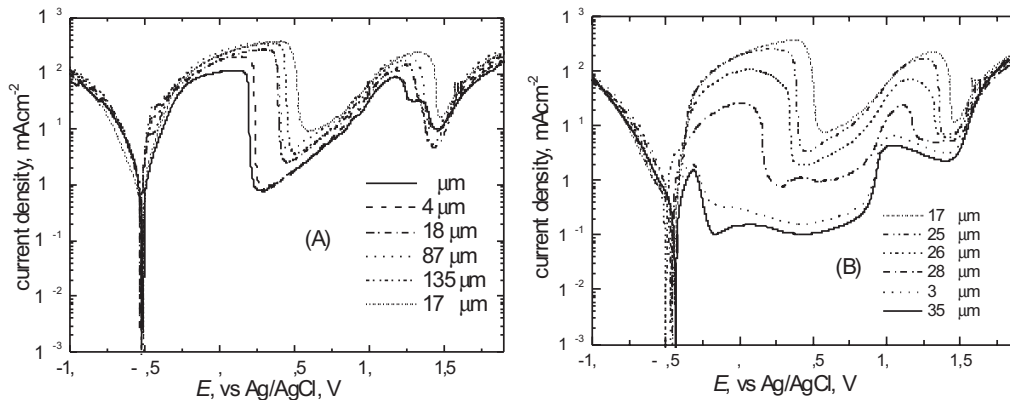


Fig. 4. Potentiodynamic polarization curves of the nitrided AISI 321 stainless steel measured for different depths from the surface. Experimental conditions: 0.5 M sulphate solution, pH = 1, temperature: $25 \pm 0.1^\circ\text{C}$, stirring rate: 12 rps, potential scan rate: 10 mVs^{-1}

By taking off successive surfacial layers and performing their electrochemical analysis, characteristic changes in corrosion parameters read from the polarization curves are possible to register. On the basis of these changes, which occur within the entire layer, depth profiles of these parameters can be plotted. In Fig.5 the most important corrosion parameters of the tested nitrided steel: corrosion current (i_{cor}), critical passivation current (i_{cp}) and minimal current in passive region ($i_{\text{min,p}}$) are presented as a function of the distance from the initial surface.

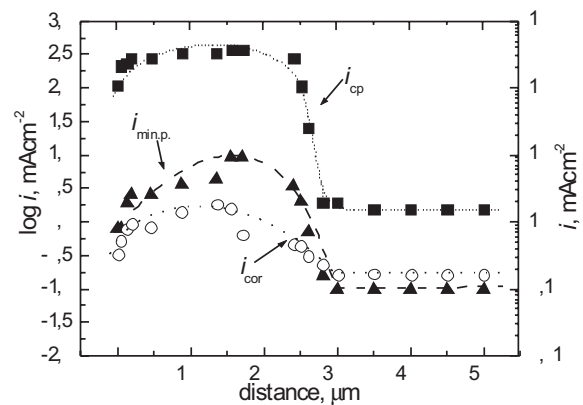


Fig. 5. Depth profiles of fundamental corrosion parameters of nitrided

AISI 321 stainless steel read from polarization curves. Experimental conditions – see Fig. 4

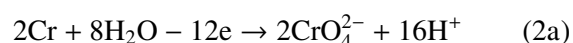
As it results from Fig.5, the most outer layers (containing nitride compounds, like CrN) exhibit moderate values of i_{cor} and $i_{min,p}$ which increase for deeper situated layers. At the depths of 100-150 μm (nitride precipitates area) these parameters show maximal values and are 5-8 times greater than these for the bulk steel. For the depths of 200-260 μm the rapid decrease of i_{cor} and $i_{min,p}$ are observed and for *ca* 300 μm they fix on constant level, typical for the bulk steel. Especially strong decrease is visible for maximum anodic current in active state (critical passivation current: i_{cp}) which is two orders of magnitude greater for the depths of 30-250 μm than that for the bulk steel.

Outer CrN-based layer possess some passivation properties owing to great amounts of chromium in it and the passivation most probably consists in the following reaction:

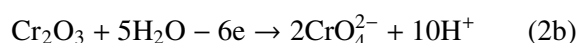


The chromium hydroxide layer is, however, porous, contains some Fe(OH)₃ deposit and, generally, does not protect of the outer layers satisfactory. On the other hand, for deeper situated layers chromium atoms are engaged in forming of nitride precipitates (mainly Cr₂N type) which strongly limits Cr concentration in austenite and consequently, the iron species (mainly Fe₃O₄ or Fe₂O₃) predominate in passive layers formed at the depths of 30-200 μm . Presence of nitride precipitates in the oxide layers increases conductivity of these layers which is prone to continuous increase of anodic currents within this “passive range” with potential increase (Fig.4, $E > 0.25\text{V}$).

At a potential of 0.9V it starts repassivation of the steel – clearly visible for the depths of 350 μm , i.e. characteristic for the bulk steel (Fig.4b – solid line). This process consists in formation high valence chromium (and nickel) ions, like CrO_4^{2-} or [5,7,8] e.g.:



or



Preferential etching of Cr (and Ni) enriches the substrate with Fe and at potentials 1.2 – 1.4V the secondary passivation takes place with formation of less protective Fe₂O₃ oxide. As it results from Fig.5, especially high

transpassive peaks correspond to depths of 100-250 μm . One should assume that chromium nitrides intensively participate at the transpassive dissolution e.g. according to the reaction:



Equilibrium potentials of reactions (2) and (3) are similar, however, exchange current for reaction (3) must have strongly predominated over the exchange current for reactions (2a) and (2b) and this is why transpassivation process is especially fast for the depths where chromium nitrides precipitate. It results from these considerations that high-temperature nitrated stainless steels will corrode with very high rates in strong oxidizing environments.

4. Concluding remarks

The application of the progressive thinning method makes it possible to plot the depth profiles of the characteristic corrosion parameters of the material subjected to high temperature nitriding treatment, practically for arbitrarily thick top layers. Enrichment of the surface of austenitic stainless steel with nitrogen impairs its resistance to general corrosion. Using the examination method applied in the present study, it is possible to register precisely any changes in the corrosion resistance of a material over the entire top layer cross-section.

The acid corrosion rate for the nitrated outer layers of the AISI 321 steel at different depths is 2-5 times greater than that of the matrix. The deterioration of corrosion resistance is much more distinct in passive and in transpassive range.

The work has been carried out in the framework of a Research Project MNiSW Nr 3T08C 042 30.

REFERENCES

- [1] F. Ashrafizadeh, Surf. Coat. Tech. **173-174**, 1196 (2003).
- [2] X. M. Zhu, M. K. Lei, Surf. Coat. Tech. **131**, 400 (2000).
- [3] C. E. Pinedo, W. A. Monteiro, Surf. Coat. Tech. **179**, 119 (2004).
- [4] A. Kagiya, K. Terakado, R. Urao, Surf. Coat. Tech. **169-170**, 397 (2003).
- [5] G. Song, Corros. Sci. **47**, 1953 (2005).
- [6] G. G. Long, J. Kruger, D. R. Black, M. Kuriyama, J. Electrochem. Soc. **130**, 240 (1983).
- [7] I. Betova, M. Bojinov, T. Laitinen, K. Makela, P. Pohjanne, T. Saario, Corros. Sci. **44**, 2675 (2002).

- [8] M. S. El-Basiouny, Brit. Corros. J. **112**, 89 (1977).
- [9] D. B. Rayaprolu, A. Hendry, J. Mater. Sci. Technol. **4**, 136 (1988).
- [10] M. Harzenmoser, R. P. Reed, HNS'90, Proc. Int. Conf., Germany, 1990.
- [11] J. Siwka, Prace Naukowe WMIM, Seria: Metalurgia **8**, s. 10, Częstochowa, 1999.
- [12] J. Mankowski, J. Flis, Corros. Sci. **35**, 111 (1993).
- [13] J. Flis, Ochr. przed Korozją, Wyd. Spec. **42**, 261 (1999).
- [14] M. K. Lei, X. M. Zhu, J. Electrochem. Soc. **152** (8), B291 (2005).
- [15] P. Sury, Brit. Corros. J. **13**, 31 (1979).
- [16] E. Skołek, J. Kamiński, T. Wierzchoń, Ochr. przed Korozją, Nr **11s/A**, 224 (2006).
- [17] M. Kuczyńska-Wydorska, J. Flis, Ochr. przed Korozją, Nr **11s/A**, 228 (2006).
- [18] Z. L. Zhang, T. Bell, Surf. Engineering **1**, 131 (1985).
- [19] E. Menthe, K. T. Rie, J. W. Schultze, S. Simson, Surf. Coat. Technology **74-75**, 412 (1995).
- [20] M. K. Lei, Z. L. Shang, J. Vac. Sci. Technol. **A15**, 421 (1997).
- [21] J. Flis, A. Gajek, J. Electroanal. Chem. **515**, 82 (2001).
- [22] K. Jagielska, H. Bala, J. Jasiński, Inż. Powierzchni, **2A**, 57 (2005).
- [23] H. Bala, K. Giza, K. Jagielska, IXth International Corrosion Symposium and Exhibition, ICCP Proceedings, **1**, 123, Ankara 22-25. IX. 2004.
- [24] K. Jagielska, H. Bala, J. Jasiński, Inż. Materiałowa Nr **3**, 403 (2006).
- [25] K. Jagielska, H. Bala, Ochr. przed Korozją, **11s/A**, 219 (2006).
- [26] M. Stern, A. L. Geary, J. Electrochem. Soc. **104**, 56 (1957).
- [27] H. Bala, Electrochim. Acta **29**, 119 (1984).
- [28] X. L. Xu, L. Wang, Z. W. Yu, Z. K. Hei, Surf. Coat. Tech. **132**, 270 (2000).
- [29] A. Fossati, F. Borgioli, E. Galvanetto, T. Bacci, Corros. Sci. **48**, 1513 (2006).
- [30] M. P. Fewell, J. M. Priest et al., Surf. Coat. Tech. **131**, 284 (2000).
- [31] T. Borowski, J. Trojanowski, T. Wierzchoń. Inż. Powierzchni **3**, 21 (2005)